Food Chemistry 463 (2025) 141326

Contents lists available at ScienceDirect

Food Chemistry

journal homepage: www.elsevier.com/locate/foodchem

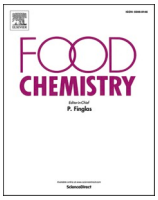

# Bioactive peptides from food waste: New innovative bio-nanocomplexes to enhance cellular uptake and biological effects

Federica Tonolo [a,*], Federico Fiorese [b], Graziano Rilievo [a], Alessandro Grinzato [c], Zahra Latifidoost [a], Ali Nikdasti [a], Alessandro Cecconello [a], Aura Cencini [a], Alessandra Folda [b], Giorgio Arrigoni [b], Oriano Marin [b], Maria Pia Rigobello [b], Massimiliano Magro [a,*], Fabio Vianello [a]

[a] Department of Comparative Biomedicine and Food Science, University of Padova, Viale dell'Università 16, 35020 Legnaro, PD, Italy
[b] Department of Biomedical Sciences, University of Padova, Via Ugo Bassi 58/B, 35131 Padova, Italy
[c] ESRF: European Synchrotron Radiation Facility, 71 Avenue des Martyrs, 38000 Grenoble, France

ARTICLE INFO

*Keywords:*
Anti-inflammatory
Antioxidant
Bioactive peptides
Food by-product
Food nanotechnology
Nanoparticles

ABSTRACT

Mastitis is the most important bovine disease, causing dramatic economic losses to the dairy industry, worldwide. This study explores the valorization of whey from cows affected by mastitis, through a novel separation approach. Surface Active Maghemite Nanoparticles (SAMNs) were used as magnetic baits to selectively bind bioactive peptides with potential health benefits. Advanced techniques such as HPLC and LC-MS/MS highlighted SAMN capability of isolating a restricted group of peptides, drastically diverging from the control profile (Solid Phase Extraction, SPE) and characterized by a peculiar acidic residue distribution. Most importantly, both magnetically purified and nano-immobilized peptides (SAMN@peptides) showed protective activity against oxidative stress and inflammation, when tested on Caco-2 cells; with SAMN@peptides being associated with the strongest biological effect. SAMNs exhibited excellent characteristics, they are environmentally sustainable, and their synthesis is cost-effective prompting at a scalable and selective tool for capturing bioactive peptides, with potential applications in functional foods and nutraceuticals.

## 1. Introduction

The demand for new and greener strategies to isolate bioactive compounds from food matrices and food by-product is increasing (Mir-Cerdà et al., 2023; Sorrenti et al., 2023). Nanotechnologies have the potential to answer this demand, and, in particular, iron oxide-based nanoparticles, such as maghemite ($\gamma$-$Fe_2O_3$) or magnetite ($Fe_3O_4$), played a crucial role in modern applications within the fields of biomedicine and biotechnology (Biswas et al., 2022; Sahani & Sharma, 2021). Among iron-oxide nanomaterials, Surface Active Maghemite Nanoparticles (SAMNs) exhibit numerous interesting properties, including superparamagnetism, high saturation magnetization, and the ability to be easily manipulated using small magnetic fields. Most importantly, they are a unique example of iron oxide nanoparticles with outstanding colloidal stability and intrinsic fluorescence, in the absence of any surface modification. Thus, SAMNs are endowed with unprecedented "dual contrast" features by being simultaneously fluorescent and magnetic (Zanin et al., 2020). Additionally, they possess favorable features, such as biocompatibility, chemical-physical stability, and low environmental impact, providing an ideal platform for the fabrication of bio-inspired hybrids.

Such bio-inspired nanomaterials were already used as drug delivery systems and biomolecule carriers, enticing the interests of the nutraceutical and pharmaceutical sectors (Fa & Zhao, 2019; Parodi et al.,

*Abbreviations:* ACN, Acetonitrile; BSA, Bovine Serum Albumin; Caco-2, Human colon-rectal adenocarcinoma cell line; DLS, Dynamic Light Scattering; DMEM, Dulbecco's Modified Eagle's Medium; FA, Formic Acid; FBS, Fetal Bovine Serum; FTIR, Fourier-Transform Infrared Spectroscopy; HPLC, High-Performance Liquid Chromatography; LC-MS/MS, Liquid Chromatography-Mass Spectrometry/Mass Spectrometry; LPS, Lipopolysaccharide; MTT, 3-(4,5-Dimethylthiazol-2-yl)-2,5-Diphenyltetrazolium Bromide; MWCO, Molecular Weight Cut-Off; PBS, Phosphate Buffered Saline; RT, Room Temperature; SAMNs, Surface Active Maghemite Nanoparticles; SPE, Solid Phase Extraction; TbOOH, *tert*-Butyl Hydroperoxide; TEM, Transmission Electron Microscopy; TNF-α, Tumor Necrosis Factor Alpha..

* Corresponding authors.
*E-mail addresses:* federica.tonolo@unipd.it (F. Tonolo), massimiliano.magro@unipd.it (M. Magro).

https://doi.org/10.1016/j.foodchem.2024.141326
Received 20 February 2024; Received in revised form 28 August 2024; Accepted 15 September 2024
Available online 18 September 2024

2017). Quite importantly, previous studies already established SAMNs marked preference for binding selected food proteins (Magro et al., 2018). This binding selectivity was contingent upon the composition of the protein environment, thereby resulting in distinct profiles of associated proteins. Consequently, SAMNs can efficiently harvest proteins and peptides depending on the affinity for their surface.

Bioactive peptides gained significant attention in recent years thanks to their capability to exert various beneficial effects on human health, for example antihypertensive, opioid, antioxidant, and anti-inflammatory (Akbarian et al., 2022; Chidike Ezeorba et al., 2024; Koirala et al., 2023; Manzoor et al., 2022;Nielsen et al., 2023; Zaky et al., 2022). In addition, it is worth to mention their potential use as ingredients for functional foods and nutraceuticals to prevent or treat several chronic conditions (Colombo et al., 2024; Manzoor et al., 2022; Rivero-Pino, 2023). Commonly, these compounds are 2–20 amino acid-long protein fragments (Nielsen et al., 2023; Zaky et al., 2022). Bioactive peptides were derived from various food sources, such as pulses, cereals, milk, meat, egg, marine products (*e.g.*, fish, prawns, or lobsters) and from food by-products (Brumă et al., 2024; Le et al., 2024; Manzoor et al., 2022; Quintieri et al., 2024; Rivero-Pino et al., 2023; Salerno et al., 2024; Song et al., 2024).

Nowadays, food science research aims to address the global challenge of food waste by providing a sustainable solution to repurpose food by-products into valuable bioactive compounds (El-Hadary et al., 2022; El-Hadary et al., 2023; Sarker et al., 2024). Indeed, different molecules from agri-food waste, such as bioactive peptides, could be reused as dietary supplements with beneficial effects on humans (Colombo et al., 2024). Bioactive peptides were generated by different processes, such as chemical or enzymatic hydrolysis, microbial fermentation, or using innovative techniques (Naeem et al., 2022).

In this work, SAMNs were used for the valorization of food industry by-products and, specifically, as an innovative approach to selectively isolate bioactive peptides from whey from cows affected by mastitis, marking a novel application in the field of food science in line with circular economy principles. This pathology is the most common disease of dairy cattle and it involves the inflammation of the mammary gland that leads to abnormal and decreased milk production (Cheng & Han, 2020). This milk must be discarded and cannot be used for further processes or for human or animal consumption, resulting in important economic losses (Guzmán-Luna et al., 2022).

The selective purification of bioactive peptides using SAMNs represents a significant advancement over traditional methods, providing greater specificity and enhanced biological activity. The dual functionality of the SAMN-peptide complexes, which combine therapeutic and diagnostic potentials, highlights the interdisciplinary nature of this research, bridging the fields of food science, nanotechnology, and molecular biology. In this view, SAMN biocompatibility was extensively demonstrated *in vitro*, using both prokaryotic and eukaryotic cells, as well as *in vivo* (Rilievo et al., 2024). Moreover, SAMN synthesis responds to crucial requirements, such as ready industrial-transfer as well as environmental sustainability and affordability (*i.e.*, below 3 USD $g^{-1}$ at laboratory scale) (Rilievo et al., 2024). Thus, the scalable nature of the proposed strategy holds substantial industrial significance, offering a sustainable and economically viable solution for producing high-value nutraceuticals and functional foods from dairy by-products.

## 2. Materials and methods

### 2.1. Materials

Fe(III) chloride hexahydrate ($FeCl_3.6H_2O$), sodium borohydride ($NaBH_4$), ammonia solution (35 % in water), sodium chloride, potassium chloride, manganese chloride, sodium nitrate, hydrochloric acid, and sodium hydroxide were purchased from Merck (Italy) at the highest commercially available purity and were used without further treatments. Ultrapure water was obtained from a Genie Direct-Pure system (RephiLe Bioscience Ltd., Shanghai, China) with a resistivity of at least 18.0 MΩ cm. Dulbecco's modified Eagle's medium (DMEM), fetal bovine serum (FBS) and penicillin-streptomycin were obtained from Gibco (Thermo Fisher Scientific, Massachusetts, USA). 2,5-Diphenyl-2H-tetrazolium bromide (MTT) was obtained from Sigma-Aldrich (St Louis, MO, USA).

### 2.2. Colloidal surface active maghemite nanoparticle (SAMN) preparation

SAMN synthesis was carried out as described in a recent publication (Rilievo et al., 2024). After synthesis, a stable colloidal stock suspension with a final concentration of 1 g $L^{-1}$ SAMNs was obtained upon nanoparticle sonication in milliQ grade water for 20 min at 50 kHz, 100 W in LBS1 ultrasonic bath (Falc Instruments, Italy). A series of Nd-Fe-B magnets (N35, 263–287 kJ $m^{-3}$ BH, 1170–1210 mT flux density by Powermagnet - Germany) was used for the nanoparticle magnetic control.

### 2.3. Preparation of whey samples

#### 2.3.1. From whole milk to whey samples

Bovine milk from cows affected by mastitis, called M throughout the manuscript, and from healthy cows, H, were obtained from "Azienda agraria sperimentale Lucio Toniolo" (University of Padova). Fresh milk samples were subjected to centrifugation at 4000 *g* for 15 min at 4 °C, following an established protocol (Magro et al., 2018). This centrifugation process separated fat from the aqueous part of the milk. Skimmed milk samples were then further processed by ultracentrifugation at 100,000 *g* for 30 min at 4 °C. At the end, the supernatant containing whey proteins and peptides was collected, and carefully filtered through Chr 1 paper filters (Millipore, Burlington, MA, USA) to further eliminate the remaining lipids. Samples were stored at −80 °C until their use.

#### 2.3.2. Protein content determination

In order to properly dilute the samples for the next steps, protein content in milk whey obtained from M or H was determined using Bradford method. Briefly, 0.01 mL whey was reacted with 0.09 mL Bradford reagent for 5 min at room temperature (Bradford, 1976). Then, the absorbance at 595 nm was acquired using a Cary 60 UV–Vis spectrophotometer (Agilent, St Clara, California, USA). The obtained values were fitted with a standard curve, built with BSA, and protein concentration was determined.

#### 2.3.3. Peptides concentration determination

Before SAMN binding, proteins and peptides with a molecular weight higher than 10 kDa were removed from the samples using Vivaspin® 20 centrifugal concentrator (10,000 MWCO polyethersulfone, Sartorius, Germany) following the manufacturer instructions (Abbasi et al., 2022; Magro et al., 2018). Milk whey was diluted with 0.5× phosphate buffered saline (PBS), to a final concentration equal to 2.5 mg $mL^{-1}$. Diluted solutions were transferred to Vivaspin® 20 and subjected to centrifugation (4000 *g*) at 4 °C for 40 min. Upon completion of the centrifugation process, filtered samples were collected and subsequently stored at −20 °C, until their use.

### 2.4. Isolation of peptides using SAMNs to produce SAMNs@peptides complexes

Concentrated milk samples from H or M were subjected to SAMN binding in a sterile environment. SAMNs were suspended in 10 mL milk whey solution, reaching 0.5 mg $mL^{-1}$ nanoparticle final concentration (Magro et al., 2018), and incubated for 1 h under orbital rotation at 4 °C to favor the formation of SAMNs@peptides complexes. Subsequently, samples were washed with 1× PBS three times to remove unbound peptides. After the washing steps, a 2 M ammonia solution was added to

the SAMNs@peptides and placed under orbital rotation at 4 °C for 1 h to separate peptides from SAMNs. Subsequently, the supernatant containing the isolated bioactive peptides was separated from SAMNs using a magnet and lyophilized (Edwards Vacuum, Burgess Hill, UK), to eliminate ammonia.

### 2.5. Solid phase extraction (SPE) of bioactive peptides

Solid Phase Extraction (SPE) was performed using a STRATA C18 column (Phenomenex, Torrance, California, USA) to isolate peptides and compare the extraction results carried out with SAMNs. A step-gradient chromatography, using increasing concentrations of acetonitrile (ACN, 5 %, 30 %, and 50 %), was carried out following the protocol outlined by Tonolo et al., 2020. The fraction obtained eluting the samples with 5 %–30 % ACN gradient were lyophilized and further analyzed due to their high peptide content.

### 2.6. HPLC analysis of the isolated peptide fractions

Fractions extracted using the SPE procedure (5–30 % ACN) along with the solutions containing potential bioactive peptides obtained with SAMNs were subjected to HPLC analysis in an Alliance 2695 apparatus connected with a PDA 996 detector (Waters, Milford, MA, USA) (Tonolo et al., 2020). Dry SPE-eluted peptides (50 μg) were resuspended in ultrapure $H_2O$ and loaded in an Onyx monolithic C18 column (Phenomenex, Torrance, CA, USA). Peptides were eluted monitoring the relative absorbance signal at 220 nm and using the following conditions: 1.8 mL $min^{-1}$ flow rate, linear gradient from 0 % to 48 % ACN/0.085 % TFA in 18 min, and a 28 min total run time. 1 mg of dry SAMN-obtained peptides from each H or M were resuspended in ultrapure $H_2O$ and loaded in a Jupiter C18 column (250 × 4.6 mm, 5 μm, 300 Å). Peptides were eluted monitoring the signal at 220 nm and using the following conditions: 1 mL $minute^{-1}$ flow rate, linear gradient from 5 % to 50 % ACN/0.085 %TFA in 30 min, and a 47 min total run time.

### 2.7. Identification of peptides by LC-MS/MS analysis

MS analyses were performed using an LTQ-Orbitrap XL mass spectrometer (Thermo Fisher Scientific, Waltham, MA, USA) coupled online with a nano-HPLC Ultimate 3000 (Dionex-ThermoFisher Scientific, Waltham, MA, USA) (Panchaud et al., 2012). Lyophilized samples (1 μg) were dissolved in $H_2O$/0.1 % formic acid (FA)/3 % ACN and subjected to LC-MS/MS analysis, using a 10 cm homemade PicoFrit® chromatographic column (75 μm internal diameter, 15 μm tip, New Objective, Littleton, MA, USA) packed with C18 material (Aeris Peptide 3.6 μm XB-C18, Phenomenex, Torrance, CA, USA), following a protocol previously reported by Tonolo et al., 2024. A linear gradient from 3 % to 40 % of ACN, 0.1 % FA in 20 min at a flow rate of 250 nL $min^{-1}$ was chosen for peptide elution from the original sample. Data obtained through LC-MS/MS analyses were elaborated using Proteome Discoverer Software (version 1.4, Thermo Fisher Scientific, Waltham, MA, USA) connected to the Mascot Search engine (version 2.2.4, Matrix Science, London, UK) against the UniProtKB database (*Bos taurus* section, version January 2023) concatenated with a database of common contaminants found in proteomic experiments. Peptide and fragment tolerances were set at 10 ppm and 0.6 Da, for the unrestricted search (no enzyme). All peptides identified by LC-MS/MS analyses were reported in the Supplementary Material Section 1.

### 2.8. In silico analysis of SAMN-peptide affinity

SAMN-peptide affinity was predicted using a fragment transformation method with an Fe(III) ion binding template, evaluating the amino acid binding potential, *i.e.* the affinity of the amino acid for the specific ion, with Fe(III) ions (C.-H. Lu et al., 2012). Before SAMN-peptide affinity evaluation, peptide 3D-folding was predicted using AlphaFold v2.3.2 (Jumper et al., 2021). As a model, four peptides with different lengths showing an *in vitro* high affinity were chosen (T-22-K, D-21-K, H-32-K, G-14-K) and one peptide with no *in vitro* specificity (*K*−22−*K*) was chosen as negative control.

### 2.9. Physical-chemical characterization of SAMN@peptides nanohybrid

The hydrodynamic radii and zeta potential values of nanohybrids and bare SAMNs were measured by dynamic light scattering (DLS) using a Zetasizer Nanoparticle analyzer ZEN3600 (Malvern Instrument, Malvern, UK).

Hydrodynamic diameters were measured for bare SAMNs and SAMN@peptides at 50 μg $mL^{-1}$ concentration in water at RT.

Zeta potential was measured at 1 mM NaCl to increase solution conductivity.

Transmission electron microscopy (TEM) images were acquired with a JEOL JEM-2010 microscope (JEOL Ltd., Tokyo, Japan) operating at 200 kV with a point-to-point resolution of 1.9 Å. TEM samples were dispersed in ethanol and treated with ultrasounds for 10 min. A drop of the diluted suspension was placed on a carbon-coated copper grid and allowed to dry by evaporation at room temperature.

Fourier transform infrared (FTIR) analyses of peptides, bare SAMNs, and SAMN@peptides were performed using an IR Affinity-1S spectrometer (Shimadzu Corp., Kyoto, Japan) equipped with a diamond ATR analyzer and LabSolutions IR software (Shimadzu Corp., Kyoto, Japan, version 2.21). The scanning range was set between 500 and 4000 $cm^{-1}$ with a resolution of 4 $cm^{-1}$ and 300 accumulated scans.

### 2.10. Effects of isolated peptides in a cellular model

#### 2.10.1. Caco-2 cells

For cellular tests, Caco-2 cells (human colon-rectal adenocarcinoma) were cultured in DMEM (Dulbecco's Modified Eagle's Medium) supplemented with 10 % fetal bovine serum (FBS) and maintained at 5 % $CO_2$ and 37 °C. The Caco-2 cell line, derived from human intestinal adenocarcinoma, is a valuable tool for studying the absorption and transport of nutrients and drugs across the intestinal epithelium. The polarized structure of these cells, with brush borders on the luminal side and a smooth basolateral membrane on the opposite side, resembles the human gut mucosa (Iftikhar et al., 2020).

#### 2.10.2. Cell viability assay

To evaluate the effects of isolated peptides on cell viability, oxidative stress or inflammation was induced in peptide-treated cells and subjected to a viability test. Briefly, Caco-2 cells ($1 \times 10^4$) were seeded in 96-well plates (Tonolo et al., 2024) and, after 48 h, cells were treated with 0.05 mg $mL^{-1}$ of each peptide sample (H or M) isolated by SPE and SAMNs or 0.01 mg $mL^{-1}$ of SAMN@peptides (H or M). After 24 h, the medium was removed and replaced with 0.5 mg $mL^{-1}$ MTT solution. Then, cells were incubated at 37 °C for 3 h in the dark. Subsequently, the MTT solution was replaced with isopropanol/dimethyl sulfoxide solution (9:1) to stop the reaction, followed by an incubation at 37 °C for 15 min. The UV–Vis absorbances at 595 and 690 nm were measured using a plate reader (Tecan Infinite® M200 PRO, Männedorf, Switzerland).

To induce oxidative stress, cells were incubated with 250 μM of TbOOH for 18 h. Inflammation was promoted using 0.01 mg $mL^{-1}$ LPS (lipopolysaccharide, Sigma-Aldrich) or 4 ng $mL^{-1}$ TNF-α (tumor necrosis factor, Sigma-Aldrich), for 18 h or 2 h, respectively.

#### 2.10.3. Cell uptake and imaging of SAMN@peptides

Caco-2 cells were seeded ($40 \times 10^4$ cells/well) upside-down onto 13 mm coverslips in 12-well plates, 48 h prior to a 24 h-incubation with 0.01 mg $mL^{-1}$ of either SAMN@H or SAMN@M. After incubation, cells were rinsed twice with PBS to remove the excess of SAMNs, and fixed with 2 % paraformaldehyde at 4 °C for 30 min. Then, cells were washed again twice with PBS and incubated with 1:1000 Hoechst (Merck KGaA,

Darmstadt, Germany) and 1 μM CellTracker Red CMTPX (Invitrogen, Waltham, MA, USA) at 37 °C for 30 min at RT. After two 30 min washes with PBS, the coverslips were mounted onto microscope slides (VWR International, Radnor, PA, USA) with Mowiol (Calbiochem, San Diego, CA, USA). Images were acquired with a Leica TCS SP5 confocal microscope equipped with a Leica HCX PL APO 40×/1.25–0.75 Oil CS objective (Zanin et al., 2020).

### 2.11. *In silico analysis of the physical-chemical properties of the identified bioactive peptides*

The physical-chemical characteristics of the identified bioactive peptides were analyzed using various bioinformatic tools: Expasy-Compute pI/MW (https://web.expasy.org/compute_pi/) and Prot-Param (https://web.expasy.org/protparam/) were used to estimate the molecular weight, the isoelectric point, the abundance of each amino acid, and the total number of positively/negatively charged residues (Wilkins et al., 1999); PepDraw server (http://www.tulane.edu/~biochem/WW/PepDraw/) was used to evaluate the net charge and the hydrophobicity of the peptides.

### 2.12. *Statistical analysis*

Values were indicated as mean ± SD of at least three independent experiments. The statistical analyses were performed by the one-way ANOVA test with a multiple comparison test through the Tukey-Kramer method and results with $p < 0.05$ were considered as statistically significant as previously reported in Tonolo et al., 2024. OriginPro software (OriginLab Corporation, Northampton, MA, USA) was used for the analysis.

## 3. Results and discussion

### 3.1. *Composition of the hybrid nanomaterial bio-coronas*

Upon exposure to a biological matrix, a nanomaterial becomes coated by biomolecules, such as proteins and peptides, developing a shell that can be generically named bio-corona (*e.g.* protein corona, peptide corona, *etc.*). The investigation of this bio-corona formation is, on one hand, important for the development of an appropriate purification strategy, and it is also fundamental for laying the basis for producing novel nano-bio-conjugates for theranostic applications. Indeed, the endowment of inorganic nanomaterials with a bio-like behavior represents a crucial task that can be obtained by integration with functional biomolecules, leading to novel pseudo-biological entities (Martinez-Veracoechea & Frenkel, 2011). In this view, SAMNs are able to recognize specific biomolecules in a complex biological milieu, forming a bio-corona characterized by a restricted composition of bio-compounds. Surface recognition properties of SAMNs were attributed the to the chelation of surface Fe(III) sites by sterically compatible carboxylic groups, exposed by proteins and peptides. Thus, with the idea of fabricating biologically active nano-hybrids combining SAMNs and bioactive compounds from milk whey, a simple self-assembly approach was adopted. Naked SAMNs were incubated in two biological matrices consisting of milk whey from mastitis-affected (M) and healthy (H) cows, as a control (Fig. 1 A). The whole process, including the washing and release procedures, is described in paragraph 2.4 of the present study. The peptide content associated with the nanomaterial bio-corona

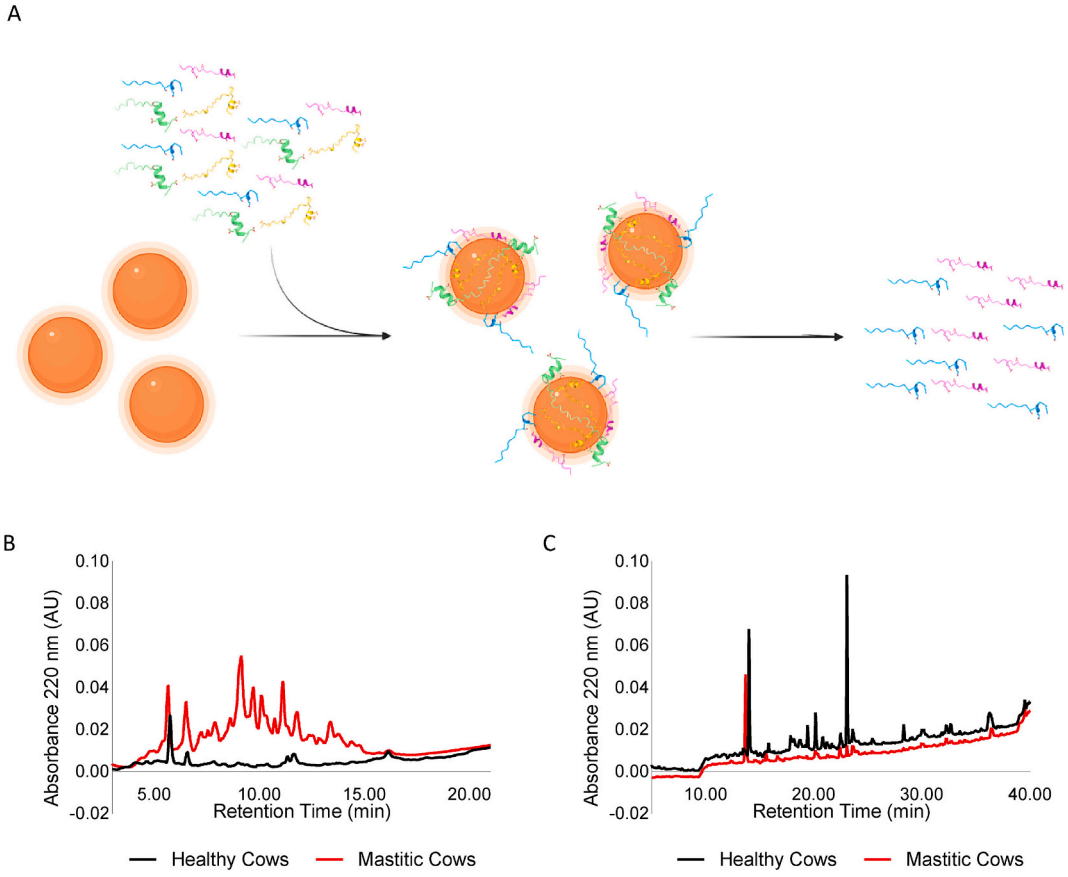


**Fig. 1.** Isolation of bioactive peptides through nanotechnological system. (A) Schematic representation of the applied method. HPLC analysis of peptides extracted by SPE (B), restricted to gradient range 3–21 min, and SAMNs (C), restricted to gradient range 5–40 min. Peptide profile of milk whey from mastitis-affected cows (M) and healthy cows (H) are reported in red and black, respectively. (For the interpretation of the references to colour in this figure legend, the reader is referred to the web version of this article.)

was analyzed using high-performance liquid chromatography (HPLC) and compared to the fractions obtained by SPE, a method commonly used for the isolation of health-promoting peptides. Briefly, SPE was carried out as reported in paragraph 2.5, using a step-gradient chromatography at increasing concentrations (5 %, 30 %, and 50 %) of acetonitrile (ACN). The fraction obtained with 5–30 % ACN gradient contained the highest concentration of peptides and, for this reason, was analyzed further.

In Fig. 1, it is possible to appreciate the significant difference between the HPLC profiles of SPE extracts (Panel 1 B) and SAMN biocoronas (Panel 1C). When compared to the chromatogram of nanoparticle cargos, the SPE-purified peptide profile appeared crowded by broad and intense signals, consistent with the scarce selectivity of the purification method with respect to the magnetic separation by SAMNs. Furthermore, SPE-peptide content isolated from M was higher with respect to H. This is due to the mastitis-induced inflammation status that stimulates proteolytic processes, releasing protein fragments, and exerting different signaling effects that trigger the defense responses of the host (Tomasinsig et al., 2010). Noteworthy, peptide recognition by SAMN showed an opposite tendency, registering a higher abundancy of isolated peptides from H samples. This could be likely ascribed to the affinity nature of the binding with SAMNs, that is mostly dependent on the amino acidic sequence and not on the mere preponderancy of the available biomolecules.

To perform an in-depth characterization of the SAMN bio-corona composition, peptides released from the colloidal nanomaterial were analyzed by LC-MS/MS and compared to SPE-obtained peptides (Table 1). The results confirmed the selectivity of SAMN surface, as evidenced by the restricted group of peptides constituting the shell of the hybrid nanomaterial (31 peptides from M samples and 16 peptides from H samples). For comparison, SPE-obtained peptide composition consisted of a *ca.* 10-fold higher number of unique peptides (306 from M and 167 from H).

Peptide size ranged from 6 to 38 amino acids, using either SAMNs or SPE, for healthy (H) and mastitis-affected (M) cows (Supplementary Material 2). The mean peptide length was slightly larger in peptides obtained using SAMNs, (21 M and 23H) than from SPE (18 M and 16H). Moreover, SAMN-isolated peptides presented a higher content of acidic residues (almost 20 %, on average, compared to *ca.* 14 % of SPE fractions). This resulted in a negative net charge of SAMN-peptides (−3, Table 1), with respect to SPE-peptides, that were generally not charged. Notably, these last molecules were rich in Proline (Pro), Lysine (Lys), Glutamic acid (Glu), and Serine (Ser), while SAMN peptides were abundant in Aspartic acid (Asp), Leucine (Leu), Glutamic acid (Glu), Glycine (Gly), and Phenylalanine (Phe). In general, peptide fractions obtained by SPE presented up to 46 % peptides with more than 50 % hydrophobic residues in their sequence (about 27 % in SAMNs fractions). Given the hydrophobic character of these compounds, it is evident that most of SPE-derived peptides, especially those from M samples, were casein fragments, specifically from α- and β-casein varieties.

Noteworthy, some peptides were unique to either the H or M whey fraction, indicating distinct peptide content profiles of these two samples. An interesting finding arises by considering that proteins shared by both fractions yielded different bioactive peptides, both in terms of quantity and of sequence (see Supplementary Material 2 for peptide grouping under the parent protein). In particular, M fractions contained a higher number of peptides, compared to the H fractions, from the same proteins.

In summary, this analysis reveals a complex and distinct peptide landscape of each fraction, highlighting the importance of determining the unique peptide content profile for a comprehensive understanding of their bioactive potential. Detailed information about the identified peptide sequences from both M and H milk, obtained by SPE and SAMNs isolation techniques, can be found in Table 1 and in the Supplementary Material 2 file.

Finally, under the reported conditions, the peptide yield resulted higher by classic SPE extraction method than by SAMN magnetic separation. The total amount of isolated peptides obtained from 100 mL of ultracentrifuged whey were 23 mg and 14 mg with SPE and SAMNs, respectively. However, on the basis of the estimated loading capacity of SAMNs (140 mg $g^{-1}$ peptide/SAMN), the amount of selectively captured peptides can be considerably augmented by simply increasing SAMN concentration during whey incubation. Indeed, it is likely to expect a linear increase of the amount of captured peptides in the nanoparticle concentration interval comprised between 100 mg $L^{-1}$ and 1 g $L^{-1}$. Thus, although the comparison with SPE performances was not the main focus of the present contribution, the use of SAMNs as purification tool can represent a viable option in terms of yield and, of course, in terms of specificity.

### 3.2. Physical-chemical characterization of SAMN@peptides complexes

To provide direct structural information regarding bio-corona formation, the hybrid nanomaterials (SAMN@H and SAMN@M) were morphological characterized by transmission electron microscopy (TEM). In Fig. 2A and B, TEM micrographs showed spherical core-shell structures displaying a bulky, less electron-dense envelope around the well-preserved maghemite core. The organic matrix displaying a thickness of approximatively 2 nm, can be attributed to the self-assembled

**Table 1**
*In silico* evaluation of the physical-chemical properties of the bioactive peptides present in the studied fractions.

| | Number of identified peptides | Number of specific peptides in each fraction | Peptide Length (mean) | Basic aa (mean %) | Acidic aa (mean %) | Neutral aa (mean %) | Hydrophobic aa (mean %) | Peptides with more than 50 % of hydrophobic aa (%) | Net charge (mean) | The most abundant aa |
|---|---|---|---|---|---|---|---|---|---|---|
| SPE M | 306 | 230 | 18 | 13 | 13 | 29 | 45 | 46 | −0.3 | Glu, Lys, Leu, Asn, Pro, Gln, Ser, Val |
| SPE H | 167 | 87 | 16 | 13 | 15 | 29 | 43 | 32 | −0.7 | Ala, Glu, Lys, Leu, Pro, Ser, Thr, Val |
| SAMNs M | 31 | 20 | 21 | 8 | 19 | 34 | 40 | 29 | −3 | Ala, Asp, Glu, Phe, Gly, Ile, Leu, Ser, Thr, Val |
| SAMNs H | 16 | 5 | 23 | 7 | 19 | 33 | 41 | 25 | −3 | Ala, Asp, Glu, Phe, Gly, Ile, Leu, Ser, Thr, Val |

SPE: Solid phase extraction; SAMNs: Surface Active Maghemite Nanoparticles; M: Milk whey from mastitis-affected cows; H: Milk whey from healthy cows; Lys: Lysine; Leu: Leucine; Pro: Proline; Gln: Glutamine; Ala: Alanine; Glu: Glutamic acid; Ser: Serine; Thr: Threonine; Val: Valine; Asp: Aspartic acid; Gly: Glycine; Ile: Isoleucine.

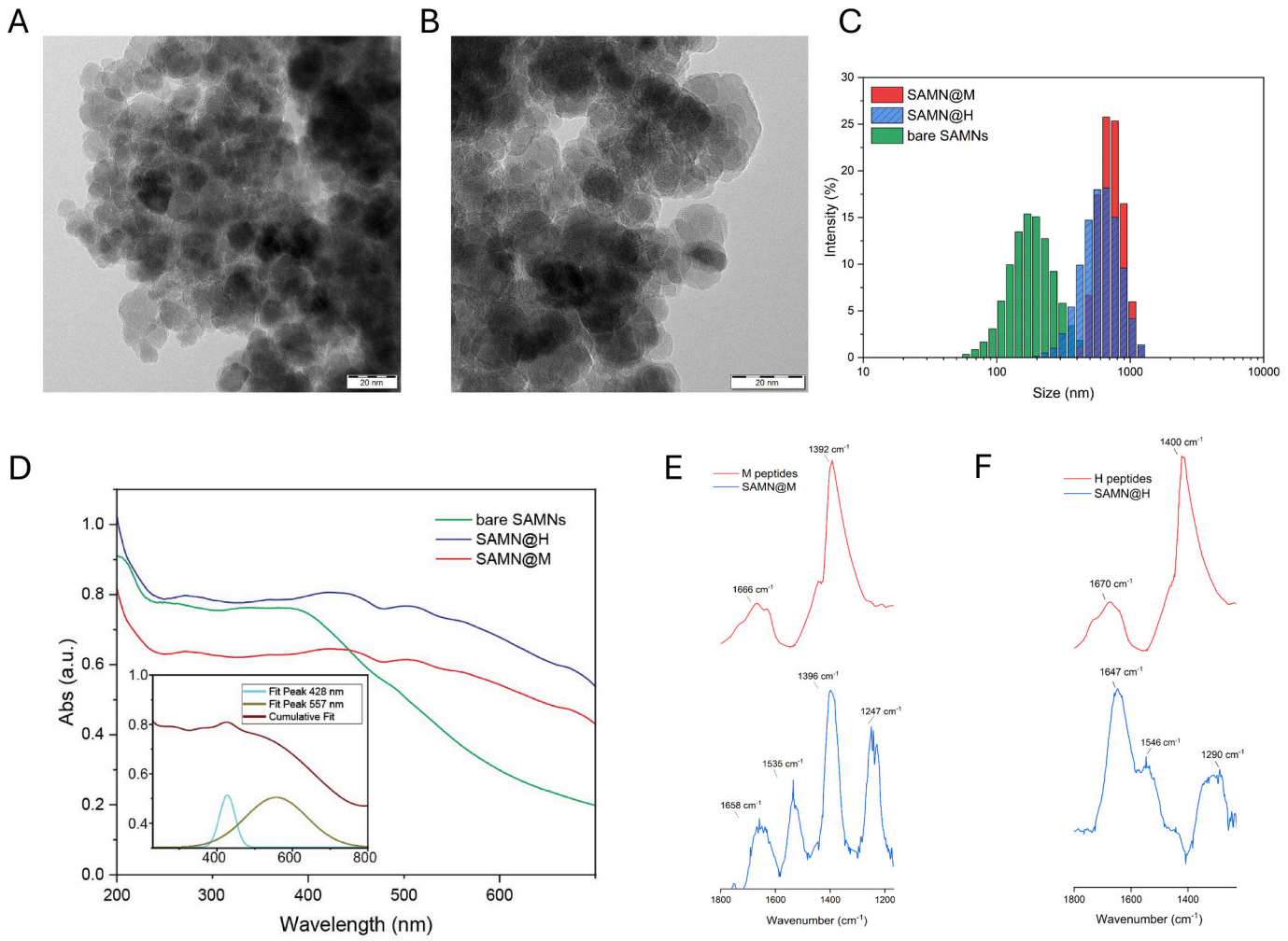


**Fig. 2.** Chemical–physical and morphological characterization of SAMN-peptide nano-hybrids. A) and B) TEM micrographs of SAMN@H and SAMN@M, respectively; C) DLS measurements with the statistical fitting according to the LogNorm function, green bars for bare SAMNs, blue bars for SAMN@H and red bars for SAMN@M; D) UV-VIS spectra of naked SAMNs, SAMN@H and SAMN@M, Inset: deconvolution of SAMN@M UV-VIS spectrum; E) and F) FT-IR spectra of nano purified peptide fractions compared to the ones of nano-immobilized peptides from M and H, respectively. (For the interpretation of the references to colour in this figure legend, the reader is referred to the web version of this article.)

peptide shell. Furthermore, the hydrodynamic features of the two nanohybrids were assessed (see Section 2) along with zeta potential (ζ) measurements resulting in the ζ value of the bare SAMNs being equal to $+30 \pm 2$ mV (conductivity = 0.113 mS cm$^{-1}$ at 25 °C), while the ζ values of SAMN@H and SAMN@M were $-6 \pm 1$ mV and $-10 \pm 1$ mV, respectively (conductivity = 0.242 and 0.226 mS cm$^{-1}$ at 25 °C). It is worth mentioning that the observed shift to negative values is compatible with the expected coordinative nature of the peptide-SAMN interaction where negatively charged acidic peptides bind to the otherwise positively-charged SAMNs. As showed in Fig. 2C, the hydrodynamic radii of SAMN@H (blue bars) and SAMN@M (red bars) were 0.90 ± 0.06 μm and 1.2 ± 0.2 μm, respectively, whereas the value for bare nanoparticles resulted equal to 0.19 ± 0.02 μm (Fig. 2C, green bars).

SAMN@H and SAMN@M complexes were further characterized by UV–Vis. In Fig. 2D, the binding of M and H peptides to SAMNs induced a *ca.* 50 nm redshift of the SAMN absorption band, accompanied by the appearance of a shoulder at 504 nm, confirming the expected complexation of under-coordinated iron(III) by the peptide chelating moieties, very likely aspartic and glutamic carboxyl groups. Interestingly, upon subtraction of the naked SAMN spectrum from the hybrid nanomaterials spectrum (Fig. 2D, inset), two distinctive signals at 428 and 558 nm were observed as distinctive features of the nano-bioconjugates and were ascribed to the contribution related to electron transitions associated with the surface modifier-metal oxide complex formation (Calabrese et al., 2015; Quintanar & Rivillas-Acevedo, 2013). It worth to note that at the physical edge of the maghemite nanoparticles, the crystalline domain is interrupted and, therefore, the surface exposes a distribution of Fe(III) sites, which are not entirely coordinated. Thus, the selective formation of a stable binding with the peptides is likely ascribable to the stability gained by adsorption-induced surface restructuration of the nanomaterial surface (Rilievo et al., 2024). This phenomenon is known as surface reconstruction and, generally, it is mirrored by a redshift of the nanoparticle UV–Vis absorption spectrum (Rajh et al., 2002). This optical transition is commonly observed when a charge transfer happens between a donor organic ligand (M and H peptides in the current case) and the conduction band of metal oxides, which are usually characterized by high crystallinity, dimensions below 20 nm, and a good colloidal stability. In this view, the redshift phenomenon represents a typical fingerprint of SAMN-biomolecule hybridization (Rilievo et al., 2024).

FTIR was adopted to highlight peptide binding, their structural modifications upon SAMN surface immobilization, as well as the molecular features involved in the binding (Barth, 2007). The FTIR spectra of SAMN-released native peptides (Fig. 2 E and F, red curves) showed the typical fingerprint of amide I band of proteins (1666 cm$^{-1}$ and 1670 cm$^{-1}$ for M and H, respectively), almost entirely due to the carbonyl

stretching of peptide bonds. However, the amide II band, expected in the interval from 1500 to 1600 $cm^{-1}$, and related to in-plane N-H bending and C-N stretching of peptide bonds, could not be punctually recognized, due to the overlapping with amide I. The evident peaks at 1392 $cm^{-1}$ and 1400 $cm^{-1}$ for M and H samples, respectively, towering over other peptide vibrational features, were ascribable to the symmetric stretching vibration of deprotonated carboxylate groups of aspartic and glutamic acid side chains (Barth, 2000). Although representing a necessary but not sufficient condition, the strong signal of carboxyl groups of the bio-corona components is fully in harmony with LC-MS/MS and *in silico* analysis and with the assumption that SAMN selectivity is ruled by the availability of chelating moieties on the bound biomolecule.

Noteworthy, in comparison to the spectra of native peptides, the IR vibrational contribution by carboxylate groups resulted significantly reduced for SAMN@M and SAMN@H (Fig. 2E and F, blue lines, respectively), whereas the characteristic amide bands were significantly more evident, particularly for SAMN@M. Moreover, amide I bands registered a shift from around 1670 to 1658 and 1647 $cm^{-1}$ for SAMN@M and SAMN@H, respectively, suggesting the occurrence of conformational modifications upon binding with respect to soluble peptides. This can be explained as the result of peptide folding upon their interaction with SAMNs, confirmed by the appearance of amide II bands, at 1535 and 1546 $cm^{-1}$, clearly identifiable in SAMN@M and SAMN@H spectra. This hypothesis is further corroborated by the occurrence of amide III band, at 1247 and 1290 $cm^{-1}$, absent in the IR spectra of soluble peptides (Barth, 2007). A folding rearrangement is not surprising, as disordered peptides displaying proper amino acid sequences can be forced to assume well-defined structures by binding to surfaces presenting suitably spaced anchoring sites (Mu et al., 2014). This can be the case of SAMN surface displaying a regular distribution of binding sites, that can be simplified into a square grid with a side length of 3.9 ± 0.9 Å, whose nodes are occupied by under-coordinated Fe(III) (Magro et al., 2018). In this view, IR spectrum modifications with respect to soluble peptides can be related to the involvement of carboxylic group side chains of aspartic and glutamic acid in the chelation of Fe(III) sites on SAMN surface (Barth, 2000; Sahoo et al., 2011). Thus, peptides are forced to assume an ordered structure to match the topography of Fe(III) sites, maximizing the number of coordination bindings and the contact area (X. Lu et al., 2019).

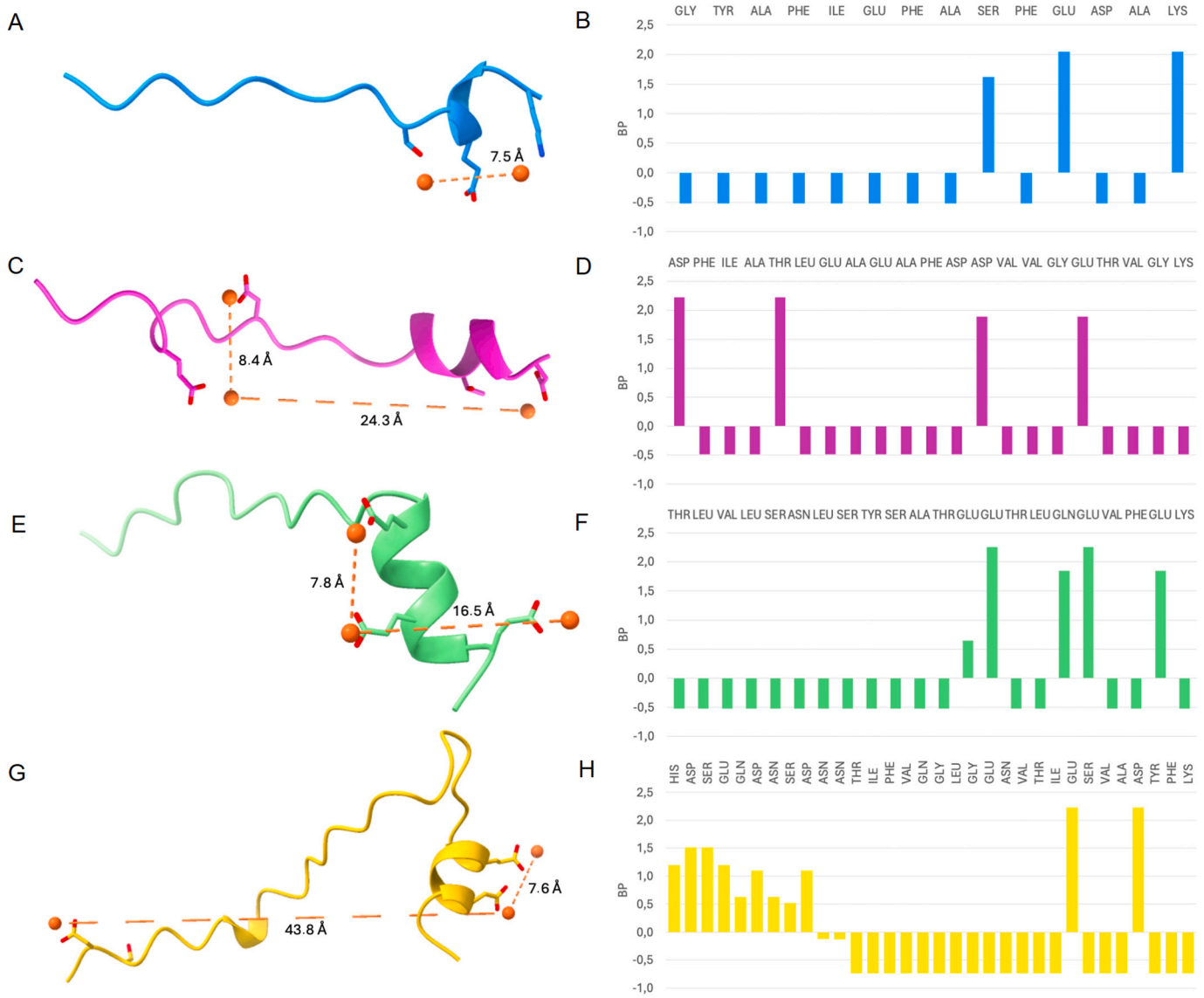


**Fig. 3.** 3D representation of SAMN-binding peptides and amino acid binding potential with Fe(III) ions of SAMNs isolated peptides. G-14-K (A,B) in cyan, D-21-K (C, D) in purple, T-22-K (E,F) in green and H-32-K (G,H) in yellow; Fe(III) ions are pictured in orange and the orange dashed line represent the distance between the Fe (III) ions, measured in Å. (For the interpretation of the references to colour in this figure legend, the reader is referred to the web version of this article.)

### 3.3. In silico evaluation of the interaction between SAMNs and peptides

Aiming at deepening the comprehension of the nanomaterial-peptide interplay, an *in silico* investigation was carried out to evaluate peptide binding potentials. Since the nanoparticles expose undercoordinated Fe (III) atoms (*vide supra*), it was assumed that these reactive sites display, in some extents, a chemical behavior comparable to soluble Fe(III) ions. In particular, Fe(III) sites are available to be coordinated by chelating ligands, such as carboxyl groups, as extensively demonstrated elsewhere, and therefore the affinity toward soluble Fe(III) can be considered for interpreting the selectivity of bio-corona formation on SAMNs (X. Lu et al., 2019). In detail, simulations showed that the carboxylate groups of Glutamic acid (Glu) or Aspartic Acid (Asn) played a crucial role in Fe(III)-peptide binding. Moreover, Glutamic acid generally exhibited a higher binding affinity compared to Aspartic Acid, and this is in line with previous studies indicating that the structural differences between these two amino acids, particularly the additional carboxyl group in glutamic acid, enhance Glutamic acid ability to stabilize Fe(III) complexes more effectively than Aspartic Acid (Shuaib et al., 2002). In Fig. 3, the structural predictions show that the presence of carboxylic groups represents a necessary but not sufficient condition to justify the binding to SAMNs. Thus, the residues that form stronger interactions with Fe(III) (*i.e.* with a binding potential over 1.5) are mainly located in peptide regions with a high tendency to form self-stable alpha helices (Fig. 3) and are separated by a regular distance (8 Å or its multiples), which is compatible with Fe(III) site distribution and, in particular, it is twice the length of the aforementioned square grid representation (*vide supra*), possibly explaining the specificity of SAMN-peptide binding (Magro et al., 2018). Therefore, this concept corroborated FTIR observations and the hypothesis that the interaction with SAMN surface would induce a further folding in those peptides displaying affinity for SAMN surface.

### 3.4. Biological effects of isolated peptides and SAMN@peptides

In order to evaluate the effects of isolated peptides on cell viability, Caco-2 cells ($1 \times 10^4$) were cultivated in the presence of 0.05 mg $mL^{-1}$ peptide fractions or 0.01 mg $mL^{-1}$ SAMNs@peptides for 24 h. As

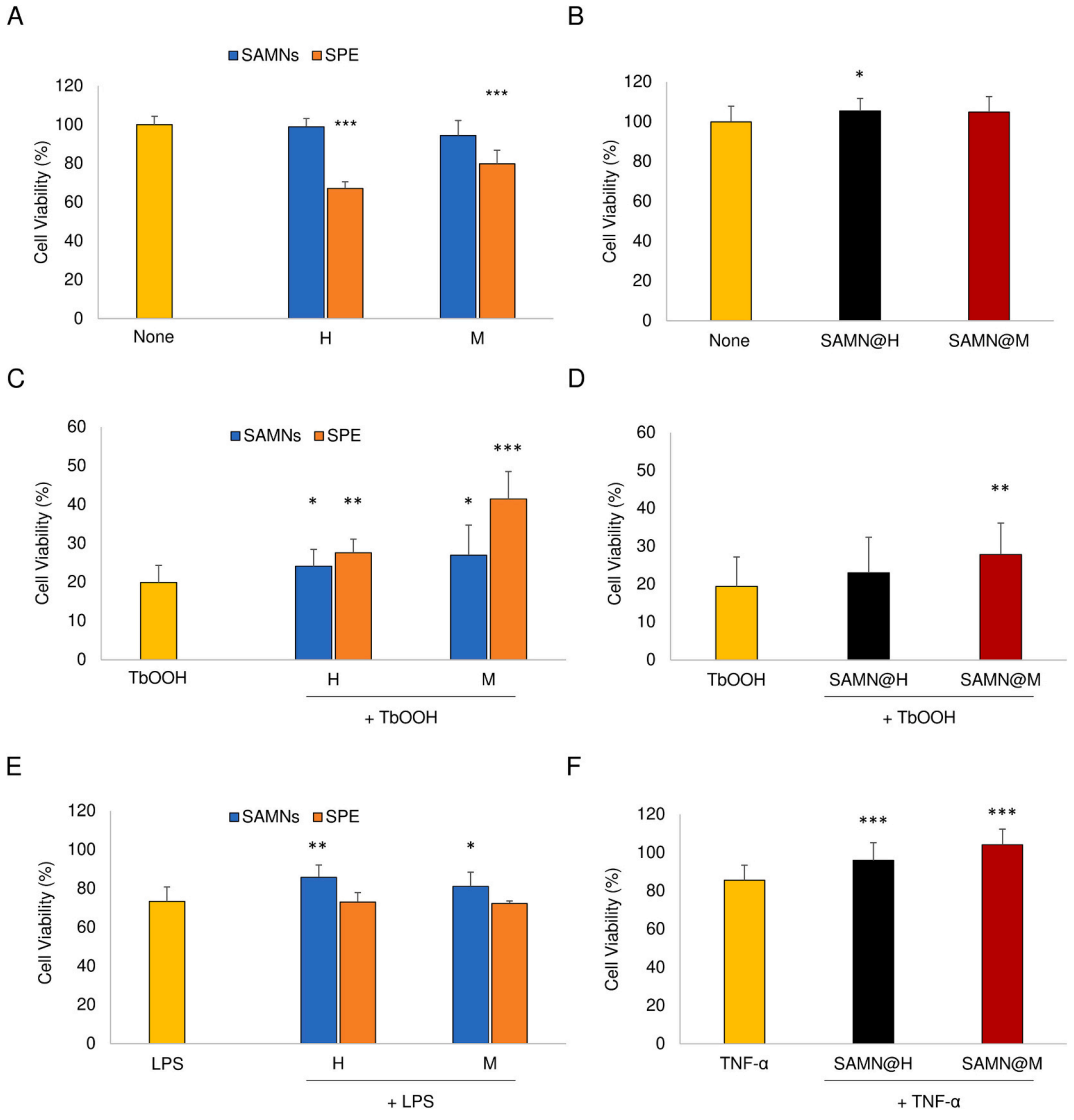


**Fig. 4.** Effects of peptide fractions extracted with SAMNs or SPE from whey of healthy (H) or mastitis-affected (M) cows and the related nanohybrids (SAMN@H and SAMN@M) on Caco-2 cell viability (A-B), against oxidative stress (C-D) and inflammation (E-F). Cell viability was evaluated by MTT assay in Caco-2 cells pre-treated with peptide fractions (0.05 mg $mL^{-1}$) or SAMN@peptides (0.01 mg $mL^{-1}$) for 24 h (par. 2.10.2). Oxidative stress or inflammation was induced by TbOOH (250 μM), LPS (0.01 mg $mL^{-1}$) or TNF-α (4 ng $mL^{-1}$) for 18 or 2 h, respectively. Data were expressed as a percentage of the values observed in untreated group. Means of at least 3 experiments were compared. *** $p < 0.001$, ** $p < 0.01$, * $p < 0.05$ *vs.* treated or untreated controls.

reported in Fig. 4A, both M and H peptides released from SAMNs displayed no harmful effects on cell viability. Conversely, SPE isolated peptides showed a decrease in cell viability. This result was attributed to the hydrophobic nature of SPE-obtained peptides. Indeed, as reported in paragraph 3.1, SPE fractions showed almost twice the amount of peptides with more than 50 % hydrophobic residues with respect to SAMN-isolated peptides. Possibly, hydrophobic peptides interact with cell membranes, potentially leading to membrane alterations and even the formation of pores, causing cell lysis.

The effects on cell viability of SAMN@peptides from milk of cows affected by mastitis (SAMN@M) and from the milk of healthy cows (SAMN@H) were tested on the same Caco-2 model. As reported in Fig. 4B, the nanohybrids (0.01 mg $mL^{-1}$) did not display any toxic effect and, on the contrary, they were beneficial. This is witnessed by a slight increase in the viability of treated cells, suggesting a non-trivial activation of specific signaling pathways as a consequence of the nanohybrids internalization.

To evaluate possible antioxidant and anti-inflammatory properties of the isolated peptides, cells ($1 \times 10^4$) were pre-treated with peptide fractions from SPE or SAMNs (0.05 mg $mL^{-1}$) and SAMN@peptides hybrids (0.01 mg $mL^{-1}$) for 24 h, and then an MTT assay was performed. Oxidative stress and inflammation were induced by 250 μM TbOOH and 0.01 mg $mL^{-1}$ LPS or 4 ng $mL^{-1}$ TNF-α, respectively, as described in the Material and Methods section. Notably, when oxidative stress and inflammation were induced in cells without any peptide treatment, cell viability decreased by 70 % and 20 %, respectively (Fig. S2). On the other hand, when cells were pre-treated with peptide fractions isolated by SPE or SAMNs, and the oxidative stress and inflammation were induced using TbOOH and LPS or TNF-α, specific effects were observed depending on each peptide fraction. In general, as reported in Fig. 4C, M-peptides showed a stronger antioxidant effect than H-peptides. Furthermore, SPE-peptides exhibited a higher antioxidant capacity in inhibiting the effects of oxidative stress induced by TbOOH, compared to those purified using SAMNs. Notably, although the concentration of nano-immobilized peptides was five-fold lower than soluble peptides, results obtained treating cells with SAMN@peptides (Fig. 4D) were comparable to the results obtained with soluble peptides (Fig. 4C). As reported in Fig. 4D, SAMN@M was able to protect cells from oxidative stress induced by TbOOH and was more effective with respect to SAMN@H.

The same trend was observed when inflammation was induced by LPS and TNF-α. As observed in Fig. 4F, SAMN@peptides exerted a strong anti-inflammatory activity against inflammation induced by TNF-α. Notably, the nanohybrids from milk of cows affected by mastitis (SAMN@M) displayed a higher anti-inflammatory capacity compared to those from milk of healthy cows (SAMN@H). Moreover, H-peptides and M-peptides, when isolated using SAMNs, demonstrated a higher anti-inflammatory capacity than those obtained by SPE (Fig. 4E).

In conclusion, SAMN-extracted peptides, despite being isolated in smaller quantities, exhibited superior bioactivity. Moreover, peptides obtained from bovines affected by mastitis showed a more antioxidant and anti-inflammatory activity than the ones from healthy cows. These results highlight that the nano-immobilized peptides provided similar or even better protection than their soluble counterparts, despite being present in lower concentrations, showcasing the efficiency of the SAMN delivery system.

### 3.5. SAMN@peptides cellular uptake

Protection against oxidative stress and inflammation mediated by SAMN@peptides suggested that these nanohybrids can enter cells and exert their action. SAMNs present an inherent green fluorescence that enables the tracking of these nanoparticles within the cells. For this reason, cells treated with SAMN@H and SAMN@M (0.1 mg $mL^{-1}$) were

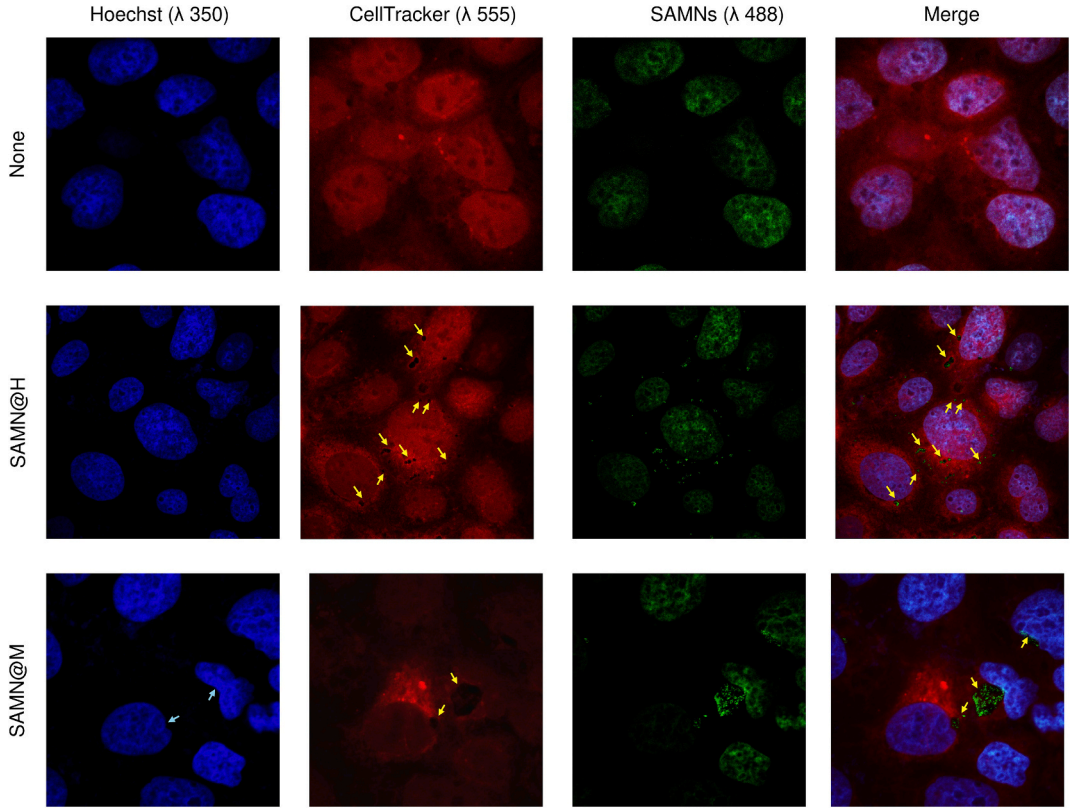


**Fig. 5.** SAMN@peptide cell uptake. Representative confocal stack images ($n = 13$) of Caco-2 cells treated with 0.1 mg $mL^{-1}$ of SAMN@M and SAMN@H for 24 h. Cells were stained with Hoechst and CellTracker RED, to highlight nuclei (blue) and cytoplasm (red), respectively. In green, SAMNs@peptides intrinsic fluorescence after excitation at λ = 488 nm. (For the interpretation of the references to colour in this figure legend, the reader is referred to the web version of this article.)

analyzed using a confocal microscope. SAMN@peptides (green) entered the cells, by a mechanism probably mediated by vesicle formation (Fig. 5). Indeed, as indicated by yellow arrows, some cytoplasmic regions in correspondence with nanoparticles are characterized by dye exclusion (CellTracker, red), suggesting the presence of a vesicle. Moreover, in cells stained for nuclei (Hoechst, blue), nanoparticle-produced organelle deformation was observed, as indicated by light blue arrows. Interestingly, the vesicles present in cells treated with SAMN@M were larger than those produced by SAMN@H, suggesting a potential difference in the interaction dynamics based on the peptide source.

Concluding, confocal microscopy revealed that SAMN@peptides entered cells predominantly through vesicle-mediated endocytosis, as evidenced by the presence of vesicles containing the nanoparticles. These observations laid the basis for understanding the nanohybrid mechanism of entrance in human cells. In addition, these results support a successful cellular uptake, while the observed intracellular effects highlight the potential of these nanohybrids as effective nutrients and drug delivery systems for therapeutic compounds, with applications in both food science and medicine.

## 4. Conclusions

A sustainable food system can bring about environmental, social, and health benefits, and offer fairer and greener economic gains (Granato et al., 2023). In the context of circular economy, different molecules present in agri-food waste could be reused as food supplements with nutraceutical effects (Granato et al., 2023). Among these compounds, bioactive peptides gained significant attention as a growing class of possible food ingredients with a wide range of potential applications (Akbarian et al., 2022; Olvera-Rosales et al., 2023; Zaky et al., 2022).

This study presents a novel method to valorize whey from mastitis-affected cows, a waste from the dairy industry, by isolating bioactive peptides using Surface Active Maghemite Nanoparticles (SAMNs). Unlike traditional methods, such as Solid Phase Extraction (SPE), which often lack specificity and result in the isolation of a broad and less targeted range of peptides, the use of SAMNs introduces a new level of specificity. SAMNs are particularly effective in isolating peptides rich in acidic residues, which are frequently overlooked by conventional methods. This selective approach represents a significant advancement in the field of peptide extraction.

Peptides immobilized on SAMNs demonstrated significant antioxidant and anti-inflammatory effects in Caco-2 cells, outperforming their soluble counterparts. This enhanced bioactivity is likely due to the improved stability and targeted delivery provided by SAMN-peptide complexes, which also showed effective cellular uptake. The unique properties of these nano-bio hybrids, including their inherent fluorescence and magnetic characteristics, further underscore their potential as multifunctional tools in both food and biomedical applications. Moreover, the scalability of this method makes it a viable option for industrial applications, offering a sustainable solution for repurposing dairy waste into valuable products.

In conclusion, this work not only provides a proof of concept for the use of SAMNs for peptide extraction but also offers new insights into the development of innovative health-promoting products. The presented interdisciplinary approach combining nanotechnology, proteomics, and molecular biology sets the stage for future research and applications in sustainable food processing and health industries.

## CRediT authorship contribution statement

**Federica Tonolo:** Writing – review & editing, Writing – original draft, Methodology, Investigation, Conceptualization. **Federico Fiorese:** Writing – review & editing, Writing – original draft, Methodology, Investigation, Formal analysis, Data curation. **Graziano Rilievo:** Writing – review & editing, Writing – original draft, Methodology, Investigation, Formal analysis, Data curation. **Zahra Latifidoost:** Writing – review & editing, Formal analysis. **Ali Nikdasti:** Writing – review & editing, Formal analysis. **Alessandro Cecconello:** Writing – review & editing, Data curation. **Aura Cencini:** Writing – review & editing, Formal analysis. **Alessandra Folda:** Writing – review & editing, Software, Investigation, Data curation. **Giorgio Arrigoni:** Writing – review & editing, Methodology. **Oriano Marin:** Writing – review & editing, Investigation. **Maria Pia Rigobello:** Writing – review & editing, Investigation. **Massimiliano Magro:** Writing – review & editing, Writing – original draft, Supervision, Resources, Project administration, Conceptualization. **Fabio Vianello:** Writing – review & editing, Writing – original draft, Resources, Project administration, Funding acquisition.

## Declaration of competing interest

The authors declare that they have no known competing financial interests or personal relationships that could have appeared to influence the work reported in this paper.

## Data availability

We have shared the obtained data as Supplementary material files.

## Acknowledgements

Federica Tonolo was supported by “iNEST- Interconnected Nord-Est Innovation ECS00000043” and and PNRR Young Researchers Project “CirculaR EConomy to enhance the sustainabilitY of agri-food Chain: An innovative approach to transform food wastE into functionaL foods”. Aura Cencini was supported by the Italian Ministry of Education, University and Research (MIUR) funds “Sentinel” and “Ecosistema dell’Innovazione”. Alessandro Cecconello was supported by REACT-EU PON “Ricerca e Innovazione 2014–2020” and STARS@UNIPD Starting Grant 2024. Authors gratefully acknowledge Jana Stráská of the Czech Advanced Technology and Research Institute (Catrin. Olomouc Czech Republic) for the electron microscopy images. The graphical abstract and part of Fig. 1 was Created with BioRender.com. We thank Dr. Maria Lina Massimino for her advice on confocal microscopy analysis.

## Appendix A. Supplementary data

Supplementary data to this article can be found online at https://doi.org/10.1016/j.foodchem.2024.141326.

## References

Abbasi, S., Moslehishad, M., & Salami, M. (2022). Antioxidant and alpha-glucosidase enzyme inhibitory properties of hydrolyzed protein and bioactive peptides of quinoa. *International Journal of Biological Macromolecules, 213*, 602–609. https://doi.org/10.1016/j.ijbiomac.2022.05.189

Akbarian, M., Khani, A., Eghbalpour, S., & Uversky, V. N. (2022). Bioactive peptides: Synthesis, sources, applications, and proposed mechanisms of action. *International Journal of Molecular Sciences, 23*(3), 1445. https://doi.org/10.3390/ijms23031445

Barth, A. (2000). The infrared absorption of amino acid side chains. *Progress in Biophysics and Molecular Biology, 74*(3–5), 141–173. https://doi.org/10.1016/S0079-6107(00)00021-3

Barth, A. (2007). Infrared spectroscopy of proteins. *Biochimica et Biophysica Acta (BBA) - Bioenergetics, 1767*(9), 1073–1101. https://doi.org/10.1016/j.bbabio.2007.06.004

Biswas, R., Alam, M., Sarkar, A., Haque, M. I., Hasan, M. M., & Hoque, M. (2022). Application of nanotechnology in food: Processing, preservation, packaging and safety assessment. *Heliyon, 8*(11), Article e11795. https://doi.org/10.1016/j.heliyon.2022.e11795

Bradford, M. M. (1976). A rapid and sensitive method for the quantitation of microgram quantities of protein utilizing the principle of protein-dye binding. *Analytical Biochemistry, 72*, 248–254. https://doi.org/10.1016/0003-2697(76)90527-3

Brumă, M., Vasilean, I., Grigore-Gurgu, L., Banu, I., & Aprodu, I. (2024). Advances in understanding the antioxidant and antigenic properties of egg-derived peptides. *Molecules, 29*(6), 1327. https://doi.org/10.3390/molecules29061327

Calabrese, I., Merli, M., & Turco Liveri, M. L. (2015). Deconvolution procedure of the UV–vis spectra. A powerful tool for the estimation of the binding of a model drug to specific solubilisation loci of bio-compatible aqueous surfactant-forming micelle.

*Spectrochimica Acta Part A: Molecular and Biomolecular Spectroscopy, 142*, 150–158. https://doi.org/10.1016/j.saa.2014.12.095
Cheng, W. N., & Han, S. G. (2020). Bovine mastitis: Risk factors, therapeutic strategies, and alternative treatments — A review. *Asian-Australasian Journal of Animal Sciences, 33*(11), 1699–1713. https://doi.org/10.5713/ajas.20.0156
Chidike Ezeorba, T. P., Ezugwu, A. L., Chukwuma, I. F., Anaduaka, E. G., & Udenigwe, C. C. (2024). Health-promoting properties of bioactive proteins and peptides of garlic (*Allium sativum*). *Food Chemistry, 435*, Article 137632. https://doi.org/10.1016/j.foodchem.2023.137632
Colombo, R., Pellicorio, V., Barberis, M., Frosi, I., & Papetti, A. (2024). Recent advances in the valorization of seed wastes as source of bioactive peptides with multifunctional properties. *Trends in Food Science & Technology, 144*, Article 104322. https://doi.org/10.1016/j.tifs.2023.104322
El-Hadary, A., Sulieman, A. M., & El-Shorbagy, G. A. (2022). Comparative the antioxidants characteristics of orange and potato peels extracts under differences in pressure and conventional extractions. *Carpathian Journal of Food Science and Technology*, 159–174. https://doi.org/10.34302/crpjfst/2022.14.1.13
El-Hadary, A., Sulieman, A. M., & El-Shorbagy, G. A. (2023). Comparative effects of Hibiscus leaves and potato Peel extracts on characteristics of fermented Orange juice. *Journal of Food Quality and Hazards Control*. https://doi.org/10.18502/jfqhc.10.1.11988
Fa, S., & Zhao, Y. (2019). General method for peptide recognition in water through bioinspired complementarity. *Chemistry of Materials, 31*(13), 4889–4896. https://doi.org/10.1021/acs.chemmater.9b01613
Granato, D., Zabetakis, I., & Koidis, A. (2023). Sustainability, nutrition, and scientific advances of functional foods under the new EU and global legislation initiatives. *Journal of Functional Foods, 109*, Article 105793. https://doi.org/10.1016/j.jff.2023.105793
Guzmán-Luna, P., Nag, R., Martínez, I., Mauricio-Iglesias, M., Hospido, A., & Cummins, E. (2022). Quantifying current and future raw milk losses due to bovine mastitis on European dairy farms under climate change scenarios. *Science of the Total Environment, 833*, Article 155149. https://doi.org/10.1016/j.scitotenv.2022.155149
Iftikhar, M., Iftikhar, A., Zhang, H., Gong, L., & Wang, J. (2020). Transport, metabolism and remedial potential of functional food extracts (FFEs) in Caco-2 cells monolayer: A review. *Food Research International, 136*, Article 109240. https://doi.org/10.1016/j.foodres.2020.109240
Jumper, J., Evans, R., Pritzel, A., Green, T., Figurnov, M., Ronneberger, O., … Hassabis, D. (2021). Highly accurate protein structure prediction with AlphaFold. *Nature, 596*(7873), 583–589. https://doi.org/10.1038/s41586-021-03819-2
Koirala, P., Dahal, M., Rai, S., Dhakal, M., Nirmal, N. P., Maqsood, S., … Buranasompob, A. (2023). Dairy milk protein–derived bioactive peptides: Avengers against metabolic syndrome. *Current Nutrition Reports, 12*(2), 308–326. https://doi.org/10.1007/s13668-023-00472-1
Le, T., Suttikhana, I., & Ashaolu, T. J. (2024). Exploring the potential applications of biopeptides from seaweeds, insects, and food wastes: Mechanisms, utilisation, and industry implications. *International Journal of Food Science & Technology, 59*(3), 1260–1267. https://doi.org/10.1111/ijfs.16920
Lu, C.-H., Lin, Y.-F., Lin, J.-J., & Yu, C.-S. (2012). Prediction of Metal Ion–Binding Sites in Proteins Using the Fragment Transformation Method. *PLoS One, 7*(6), Article e39252. https://doi.org/10.1371/journal.pone.0039252
Lu, X., Xu, P., Ding, H.-M., Yu, Y.-S., Huo, D., & Ma, Y.-Q. (2019). Tailoring the component of protein corona via simple chemistry. *Nature Communications, 10*(1), 4520. https://doi.org/10.1038/s41467-019-12470-5
Magro, M., Zaccarin, M., Miotto, G., Da Dalt, L., Baratella, D., Fariselli, P., … Vianello, F. (2018). Analysis of hard protein corona composition on selective iron oxide nanoparticles by MALDI-TOF mass spectrometry: Identification and amplification of a hidden mastitis biomarker in milk proteome. *Analytical and Bioanalytical Chemistry, 410*(12), 2949–2959. https://doi.org/10.1007/s00216-018-0976-z
Manzoor, M., Singh, J., & Gani, A. (2022). Exploration of bioactive peptides from various origin as promising nutraceutical treasures: In vitro, in silico and in vivo studies. *Food Chemistry, 373*, Article 131395. https://doi.org/10.1016/j.foodchem.2021.131395
Martinez-Veracoechea, F. J., & Frenkel, D. (2011). Designing super selectivity in multivalent nano-particle binding. *Proceedings of the National Academy of Sciences, 108*(27), 10963–10968. https://doi.org/10.1073/pnas.1105351108
Mir-Cerdà, A., Nuñez, O., Granados, M., Sentellas, S., & Saurina, J. (2023). An overview of the extraction and characterization of bioactive phenolic compounds from Agri-food waste within the framework of circular bioeconomy. *TrAC Trends in Analytical Chemistry, 161*, Article 116994. https://doi.org/10.1016/j.trac.2023.116994
Mu, Q., Jiang, G., Chen, L., Zhou, H., Fourches, D., Tropsha, A., & Yan, B. (2014). Chemical basis of interactions between engineered nanoparticles and biological systems. *Chemical Reviews, 114*(15), 7740–7781. https://doi.org/10.1021/cr400295a
Naeem, M., Malik, M. I., Umar, T., Ashraf, S., & Ahmad, A. (2022). A comprehensive review about bioactive peptides: Sources to future perspective. *International Journal of Peptide Research and Therapeutics, 28*(6), 155. https://doi.org/10.1007/s10989-022-10465-3
Nielsen, S. D.-H., Liang, N., Rathish, H., Kim, B. J., Lueangsakulthai, J., Koh, J., … Dallas, D. C. (2023). Bioactive milk peptides: An updated comprehensive overview and database. *Critical Reviews in Food Science and Nutrition*, 1–20. https://doi.org/10.1080/10408398.2023.2240396
Olvera-Rosales, L. B., Cruz-Guerrero, A. E., García-Garibay, J. M., Gómez-Ruíz, L. C., Contreras-López, E., Guzmán-Rodríguez, F., & González-Olivares, L. G. (2023). Bioactive peptides of whey: Obtaining, activity, mechanism of action, and further applications. *Critical Reviews in Food Science and Nutrition, 63*(30), 10351–10381. https://doi.org/10.1080/10408398.2022.2079113
Panchaud, A., Affolter, M., & Kussmann, M. (2012). Mass spectrometry for nutritional peptidomics: How to analyze food bioactives and their health effects. *Journal of Proteomics, 75*(12), 3546–3559. https://doi.org/10.1016/j.jprot.2011.12.022
Parodi, A., Molinaro, R., Sushnitha, M., Evangelopoulos, M., Martinez, J. O., Arrighetti, N., … Tasciotti, E. (2017). Bio-inspired engineering of cell- and virus-like nanoparticles for drug delivery. *Biomaterials, 147*, 155–168. https://doi.org/10.1016/j.biomaterials.2017.09.020
Quintanar, L., & Rivillas-Acevedo, L. (2013). *Studying metal ion–protein interactions: Electronic absorption, circular dichroism, and electron paramagnetic resonance* (pp. 267–297). https://doi.org/10.1007/978-1-62703-398-5_10
Quintieri, L., Fanelli, F., Monaci, L., & Fusco, V. (2024). Milk and its derivatives as sources of components and microorganisms with health-promoting properties: Probiotics and bioactive peptides. *Foods, 13*(4), 601. https://doi.org/10.3390/foods13040601
Rajh, T., Chen, L. X., Lukas, K., Liu, T., Thurnauer, M. C., & Tiede, D. M. (2002). Surface restructuring of nanoparticles: An efficient route for ligand−metal oxide crosstalk. *The Journal of Physical Chemistry B, 106*(41), 10543–10552. https://doi.org/10.1021/jp021235v
Rilievo, G., Cencini, A., Cecconello, A., Currò, S., Bortoletti, M., Leszczyńska, K., Górska, S., Fasolato, L., Tonolo, F., de Almeida Roger, J., Vianello, F., & Magro, M. (2024). Interactions between prokaryotic polysaccharides and colloidal magnetic nanoparticles for bacteria removal: A strategy for circumventing antibiotic resistance. *International Journal of Biological Macromolecules, 274*, Article 133415. https://doi.org/10.1016/j.ijbiomac.2024.133415
Rivero-Pino, F. (2023). Bioactive food-derived peptides for functional nutrition: Effect of fortification, processing and storage on peptide stability and bioactivity within food matrices. *Food Chemistry, 406*, Article 135046. https://doi.org/10.1016/j.foodchem.2022.135046
Rivero-Pino, F., Leon, M. J., Millan-Linares, M. C., & Montserrat-de la Paz, S. (2023). Antimicrobial plant-derived peptides obtained by enzymatic hydrolysis and fermentation as components to improve current food systems. *Trends in Food Science & Technology, 135*, 32–42. https://doi.org/10.1016/j.tifs.2023.03.005
Sahani, S., & Sharma, Y. C. (2021). Advancements in applications of nanotechnology in global food industry. *Food Chemistry, 342*, Article 128318. https://doi.org/10.1016/j.foodchem.2020.128318
Sahoo, D., Bhattacharya, P., Patra, H. K., Mandal, P., & Chakravorti, S. (2011). Gold nanoparticle induced conformational changes in heme protein. *Journal of Nanoparticle Research, 13*(12), 6755–6760. https://doi.org/10.1007/s11051-011-0583-9
Salerno, T. M. G., Coppolino, C., Arena, P., Aichouni, A., Cerrato, A., Capriotti, A. L., … Mondello, L. (2024). Circular economy in the food chain: Retrieval and characterization of antimicrobial peptides from fish waste hydrolysates. *Food Analytical Methods, 17*(2), 178–199. https://doi.org/10.1007/s12161-023-02543-z
Sarker, A., Ahmmed, R., Ahsan, S. M., Rana, J., Ghosh, M. K., & Nandi, R. (2024). A comprehensive review of food waste valorization for the sustainable management of global food waste. *Sustainable Food Technology, 2*(1), 48–69. https://doi.org/10.1039/D3FB00156C
Shuaib, N. M., Marafie, H. M., Youngo, H. B., Al-Sogair, F. M., & El-Ezaby, M. S. (2002). The binding affinity of Fe(III) to aspartic acid and glutamic acid Monohydroxamates. *Journal of Coordination Chemistry, 55*(8), 933–949. https://doi.org/10.1080/0095897022000002268
Song, L., Chen, Y., Liu, H., & Zhang, X. (2024). Preparation, biological activities, and potential applications of hen egg-derived peptides: A review. *Foods, 13*(6), 885. https://doi.org/10.3390/foods13060885
Sorrenti, V., Burò, I., Consoli, V., & Vanella, L. (2023). Recent advances in health benefits of bioactive compounds from food wastes and by-products: Biochemical aspects. *International Journal of Molecular Sciences, 24*(3), 2019. https://doi.org/10.3390/ijms24032019
Tomasinsig, L., De Conti, G., Skerlavaj, B., Piccinini, R., Mazzilli, M., D'Este, F., … Zanetti, M. (2010). Broad-Spectrum activity against bacterial mastitis pathogens and activation of mammary epithelial cells support a protective role of neutrophil Cathelicidins in bovine mastitis. *Infection and Immunity, 78*(4), 1781–1788. https://doi.org/10.1128/IAI.01090-09
Tonolo, F., Coletta, S., Fiorese, F., Grinzato, A., Albanesi, M., Folda, A., … de Bernard, M. (2024). Sunflower seed-derived bioactive peptides show antioxidant and anti-inflammatory activity: From in silico simulation to the animal model. *Food Chemistry, 439*, Article 138124. https://doi.org/10.1016/j.foodchem.2023.138124
Tonolo, F., Fiorese, F., Moretto, L., Folda, A., Scalcon, V., Grinzato, A., … Rigobello, M. P. (2020). Identification of new peptides from fermented Milk showing antioxidant properties: Mechanism of action. *Antioxidants, 9*(2), 117. https://doi.org/10.3390/antiox9020117
Wilkins, M. R., Gasteiger, E., Bairoch, A., Sanchez, J.-C., Williams, K. L., Appel, R. D., & Hochstrasser, D. F. (1999). Protein identification and analysis tools in the ExPASy server. In H. Press (Ed.), *112. 2-D proteome analysis protocols. Methods in molecular biology* (pp. 531–552). Humana Press. https://doi.org/10.1385/1-59259-584-7:531. In: Link, A.J. (eds).
Zaky, A. A., Simal-Gandara, J., Eun, J.-B., Shim, J.-H., & Abd El-Aty, A. M. (2022). Bioactivities, applications, safety, and health benefits of bioactive peptides from food and by-products: A review. *Frontiers in Nutrition, 8*. https://doi.org/10.3389/fnut.2021.815640
Zanin, S., Molinari, S., Cozza, G., Magro, M., Fedele, G., Vianello, F., & Venerando, A. (2020). Intracellular protein kinase CK2 inhibition by ferulic acid-based trimodal nanodevice. *International Journal of Biological Macromolecules, 165*, 701–712. https://doi.org/10.1016/j.ijbiomac.2020.09.207